TEST ANALYSIS OF THREE DIMENSIONAL FOLDS IN TAPE SPRINGS FOR SPACE APPLICATIONS

Scott J. I. Walker and Guglielmo S. Aglietti
University of Southampton, UK

Abstract

There is a requirement in the current space industry (due to recent technological advances) for small satellite, area deployment devices. Such devices are used to deploy antennae and solar arrays, and demand the usual requirements of low mass, low cost and high reliability that are needed for space missions. Due to the mass reduction of small satellite missions, new systems are required to achieve these deployed areas. Scaled down versions of existing larger mechanisms would not achieve the required performance. Therefore, these systems are specifically designed and optimised for missions with a very low total mass. There has been significant research performed into using tape springs (thin metallic strips with a curved cross section) folded to form simple but effective hinges, in such deployment systems. The advantages of tape springs are clear. They have low mass, do not require lubrication and automatically locks in the deployed configuration. The past research has focused on analysing and modelling tape springs folded in two dimensions. Applications of using tape springs folded in three dimensions have now been envisaged initiating this study which focuses on analysing the dynamics of tape springs folded in this way, using both experimental and theoretical methods. A test rig has been constructed to measure both the bending and twisting moments induced by the presence of such a fold in a tape spring. This test rig is initially used to verify the moments created from a two-dimensional fold and compare these results with existing theories. The results of the three dimensional experimental tests are then presented and compared with theoretical models. The paper is concluded by discussing the future steps and advancements required to model the deployment of an array which incorporates tape springs folded in three dimensions.

NOMENCLATURE

D	Flexural Rigidity
ν	Poisson's Ratio
α	Angle subtended by cross-section of spring
t	Thickness of the tape spring
θ	Total longitudinal fold angle
γ	Total twisting fold angle
M	Bending moment applied to the strip (about y axis)
M_+^{max}	Peak moment for opposite sense bending
M_-^{max}	Peak moment for equal sense bending
M_+^*	Steady state moment for opposite sense bending
M_-^*	Steady state moment for equal sense bending
T	Transverse twisting moment
T^{max}	Maximum torsional moment
R_x	Initial longitudinal radius of curvature
R_y	Initial transverse radius of curvature
L	Length of the tape spring

1. INTRODUCTION

In recent years there has been increasing focus on small satellite technology due to the potential cost savings of low mass missions. With advances in miniature electronic and mechanical systems (MEMS) (as found in Liebe & Mobasser (2001)) it is now possible to construct satellites weighing only a few kilograms. Such development opens up many new possibilities for space exploration at low cost for a far wider community of scientists and businesses (Fleeter, 2000). It is known, however, that the satellite power requirement does not reduce linearly with mass. For example, the small size of cellular telephones and hand held receivers for the Global Positioning Satellite (GPS) navigation system creates a need for larger antenna sizes in the space-based components of the system. Greater capacity requires greater on-board power, provided by deployed solar arrays. There is also ongoing research into the use of ion propulsion systems, as primary and secondary propulsion for small satellites, due to their low mass potential (Paine & Gabriel, 2001). Such systems would also significantly increase the power requirement of the satellite. Previous small satellites have used body mounted photovoltaic solar cells to provide the power required. In an attempt to provide more power, some satellites have incorporated simple fold out panels to double or triple the area projected to the sun. However, more effective systems are required to increase the capability of small satellites. A conceptual deployment system has previously been proposed by Walker & Aglietti (2002) that is capable of producing 9 times the projected area to the sun. This system uses a blanket array that unfolds bi-axially to create the required area. The supporting structure consists of tape springs diagonally connecting the opposing corners of the array. In the un-deployed configuration the tape springs are both folded and twisted to allow the array to be mounted compactly against the satellite. The deployment dynamics of the array are therefore dominated by the dynamics of the unfolding tape springs. This study focuses on the experimental analysis of tape springs that are folded in three dimensions, with an aim to model the static and dynamic characteristics of the array deployment.

2. PROPERTIES OF TAPE SPRINGS

Tape springs are defined as thin metallic strips with a curved cross section, which have the key property that they are continuous (i.e. contain no mechanical hinges or other folding devices) and yet they can still be folded elastically (Seffen et al., 2000). The general co-ordinate system to be used in this work is shown in figure 1 and the initial tape spring geometrical properties are shown in figure 2 (see nomenclature for symbol description).

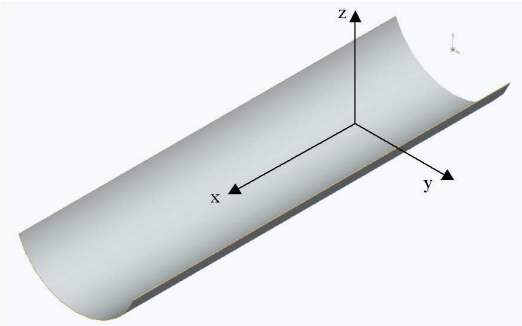

Figure 1. Tape Spring Co-ordinate System used for all Subsequent Analyses

When a tape spring of length L is loaded by equal and opposite applied moments M in the soft plane of the

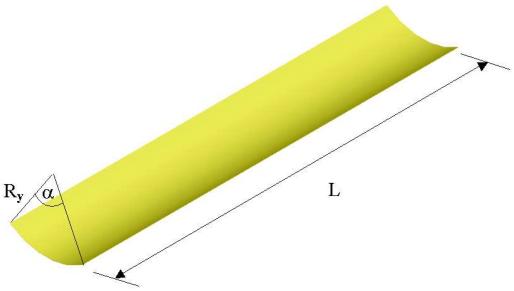

Figure 2. Initial Tape Spring Parameters

tape spring (i.e. moments about the y axis) a standard moment-rotation relationship is produced as shown in

figure 3. This relationship is the basis of two dimensional tape spring bend analysis, which attempts to predict

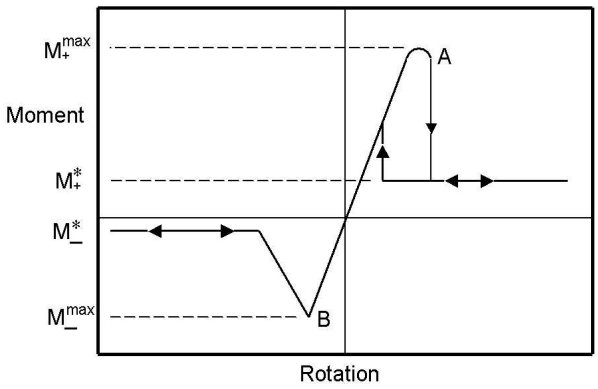

Figure 3. Graph of Moment-Rotation relationship for a two dimensional tape spring fold

the peak moments (M_+^{max}, M_-^{max}) and the steady state moments (M_+^*, M_-^*). Buckling occurs at A and B, after which localised folds form in the tape spring. It is defined that positive applied moments produce tension along the edges of the strip resulting in a longitudinal curve that is in the opposite sense to the initial transverse curve of the tape spring. This is known as an opposite sense fold. Conversely, negative applied moments create compression along the edges of the strip, resulting in equal sense folds (Seffen & Pellegrino, 1999). Opposite sense folds fail via 'snap through' buckling whereas equal sense bends fail via a torsional buckling mode. This means that opposite sense peak moments are higher than equal sense peak moments. Three separate regions

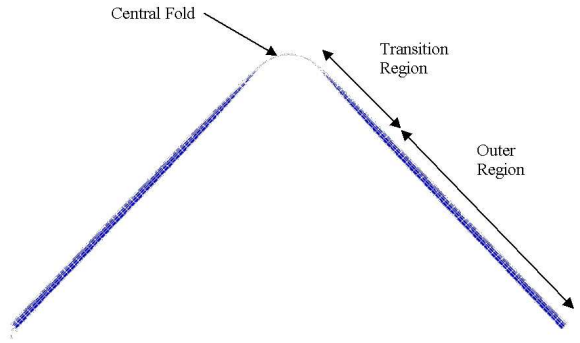

Figure 4. Regions of a post buckling tape spring fold

are defined for post buckling folds (shown in figure 4). The central fold region has a large radius of curvature that approximates a flat strip. The transition region is the length of tape spring over which the cross section returns to its initial curvature and the outer region is the length unchanged by the presence of the fold.
The longitudinal rotation of the tape spring is denoted by the symbol θ and is defined as the relative rotation of the tape spring between each end. Figure 4 therefore displays a rotation of $\theta = 90°$.
Three dimensional tape spring folds not only incorporate longitudinal rotation displacements (θ) but also relative twisting rotation between the tape spring ends, which is denoted by γ. A three dimensional fold ($\theta = 20°$, $\gamma = 40°$) is shown in figure 5. A rotating co-ordinate system for three dimensional bends is defined such that as the tape spring rotationally displaces about the y axis, the x' axis rotates to remain in the flat plane of the tape spring. The z' axis also rotates to remain perpendicular to x'. Therefore, twisting always occurs around the x' axis (see figure 6). The focus of this study is to develop a experimental test rig to determine the reaction moments about y and x'.

3. EXPERIMENT TEST RIG DEVELOPMENT

The general requirements of the experimental test rig are:

- The fixed ends of the tape spring needs to retain its initial curved geometry.

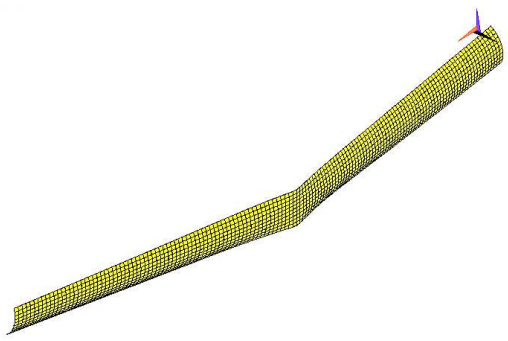

Figure 5. Simulated Three Dimensional Tape Spring Fold

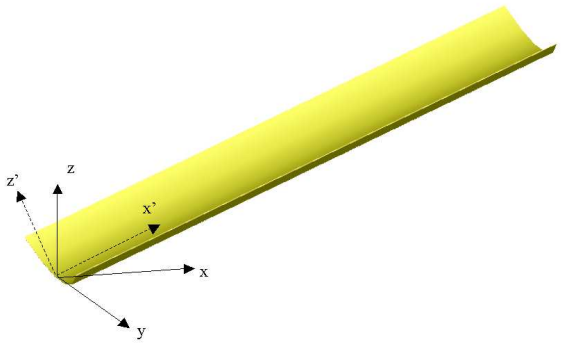

Figure 6. Rotating Co-ordinate System

- Each end of the tape spring needs two degrees of freedom of rotation (about y and x') and one clamped end needs to be free to move along x.
- The rotation about x' must be greater than 90° and the rotation about y must be greater than 45° (for each clamped end).
- Due to the highly non-linear nature of the folds, rotational displacements (not torques need to control the motion of the system.
- All the reaction moments from each axis of rotation needs to be accurately measured.

The design and layout of the experimental tests rig was initially developed around the measurement system, as this is critical to produce accurate experimental results. The magnitudes of the reaction moments vary largely between the y and x' axes and also depends greatly on the initial tape spring parameters. Therefore a measurement system was developed that allowed the system to be optimised for the anticipated moment magnitude.
The reaction moments are measured by a strain gauge unit (SGU) (shown in figure 7) that is attached between a locking level (rotationally fixed about each axle) and a torque bar (fixed to the freely rotating axle) as shown in figure 8. As a force is applied across the SGU load arms, the metal strip bends resulting in an output voltage from the strain gauge that is in proportion to the applied force. The required rotational displacements are inputted into the system through the locking level, which is rotated and locked at the desired rotation angle.
The magnitude of the load across the arms of the SGU can then be altered by either one or a combination of the following methods.

- By altering the dimensions of the test strip (thickness, width)
- By altering the radial mounting location of the strain gauge unit
- By altering the number of strain gauge units mounted around an axle

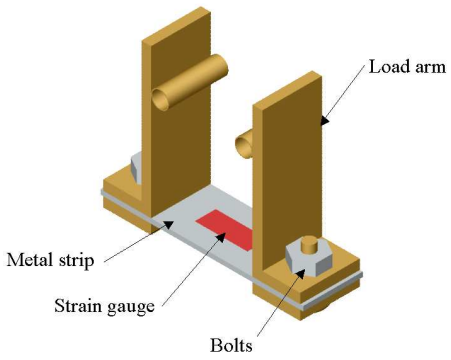

Figure 7. Strain Gauge Unit

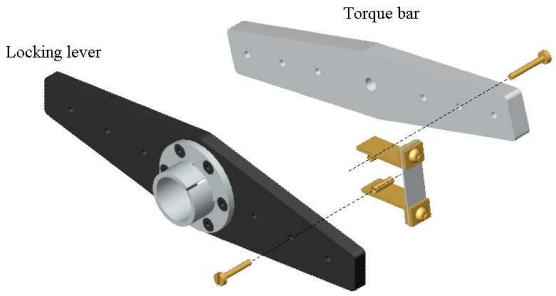

Figure 8. The Measurement System Layout

The structure for the test rig was then designed and constructed specifically to mount this system. To retain the initial geometry of the tape spring ends the clamps were specially designed to precisely match the curvature of the test strip. It was determined that in order to allow rotational freedom of the clamped end about both y and x', while preventing any unwanted linear translation of the clamped ends the y axis must be the 'dominant' rotation axis. The twist axis must therefore be mounted on a structure which rotates about the y axis (see figures 9 and 10). The height of the y axle was then designed to allow this rotating structure to freely rotate

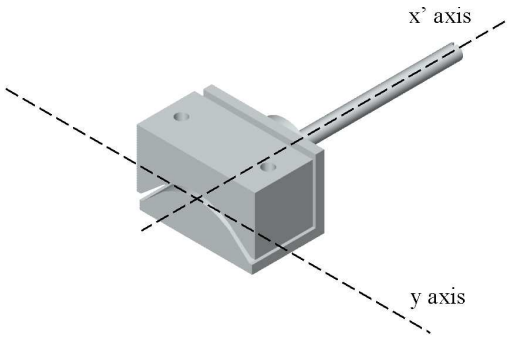

Figure 9. Required rotation of the clamped ends

$> 45°$. To ensure the rotating structure is balanced throughout the rotation, weights are mounted at the front of the structure to counter balance the weight of the measurement system. Any slight balancing inaccuracies are measured in a pretest and subtracted from the test result.
With a single translational degree of freedom required for one of the clamped taped spring ends, a moving end of the test rig was designed that uses a rail mounted carriage. The linear movement of is moving end is laterally restricted by a 'v' track which is mounted on a base board. The other clamped end structure was fixed directly to the base board allowing a maximum test strip length of just over 500mm. The total structure can be seen in figure 11, which clearly displays the fixed and moving ends of the test rig.

Temperature compensating circuits were used to minimise the magnitude of error from the strain gauges and all the data was captured statically, with 100 samples taken for each displacement step.
A photograph of the experimental test rig can be seen in figure 12.

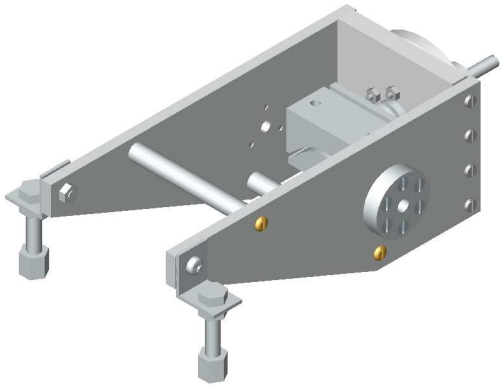

Figure 10. Rotating Structure about the Y axis

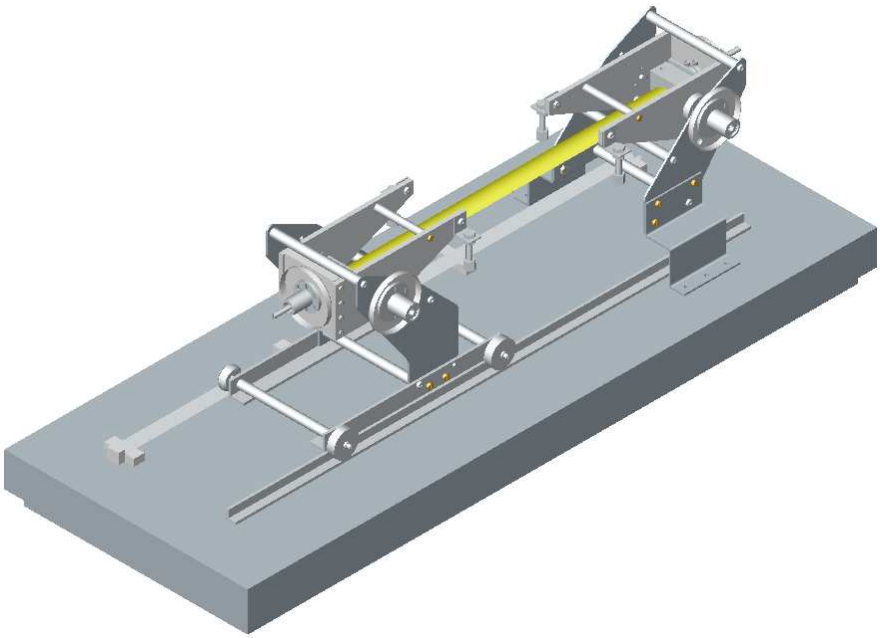

Figure 11. Total Structure of the Experimental Test Rig (measurement system not displayed)

4. TWO DIMENSIONAL RESULTS AND COMPARISONS

The initials tests were performed on a 400mm long tape spring made from 0.11mm thick, AISI 1095 steel. The tape spring had an initial transverse radius of curvature (R_y) of 20mm and an initial cross sectional angle of embrace (α) of 1.25 rad. Two dimensional bends were used to investigate the accuracy of the experimental results produced from the test rig. These test were performed using one Y SGU per axle. Each Y SGU incorporated a Nickel Silver metal strip 10mm wide, 0.8mm thick with an SGU arm length of 18mm. The two dimensional equal sense loading and unloading experimental results can be seen in figure 13. These results predict a peak equal sense moment (M_{-}^{max}) of 80Nmm and an average steady state moment (M_{-}^{*}) of 23.25Nmm. (M_{-}^{max} is found from the loading relationship as it is known that the unloading relationship results in a lower peak (Seffen et al., 2000).)

Figure 14 displays the unloading moment-rotation relationship for a two dimensional opposite sense bend. It was found that due to the experimental test increment angle of 5° per end, the peak opposite sense moment could not be determined accurately. Therefore, these initial experimental tests focused on unloading opposite sense bends. From figure 14, it can be seen that no unloading peak moment occurs. This is because the snap back occurs when $\theta < 10°$. This result predicts an average opposite sense steady state moment (M_{+}^{*}) of 41.75Nmm. To determine the accuracy of the experimental results they were compared with analytical models (derived from shell theory (Mansfield, 1973)) and finite element models. These results are shown in tables 1 and 2.

From the 2D equal sense bend results in table 1 it can be seen that the experimental results for the steady state moment are very close to the theoretically predicted values. The experimental test has an average steady

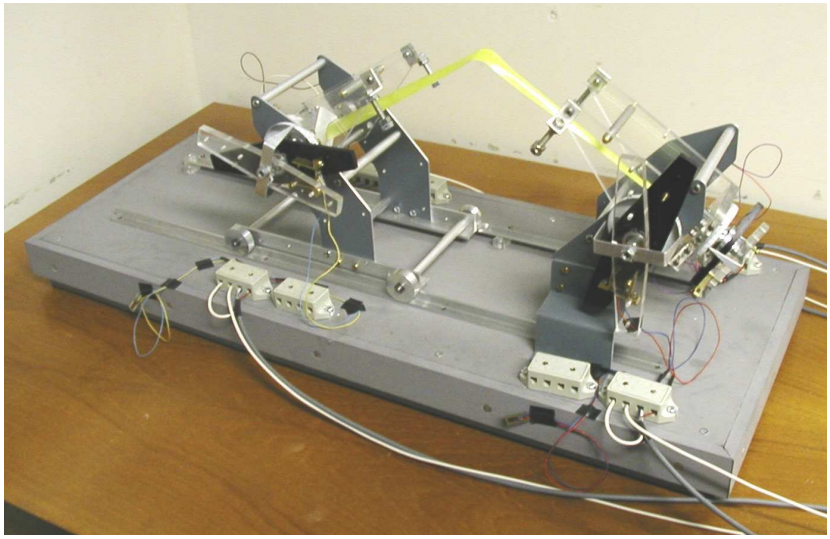

Figure 12. Photograph of the Experimental Test Rig

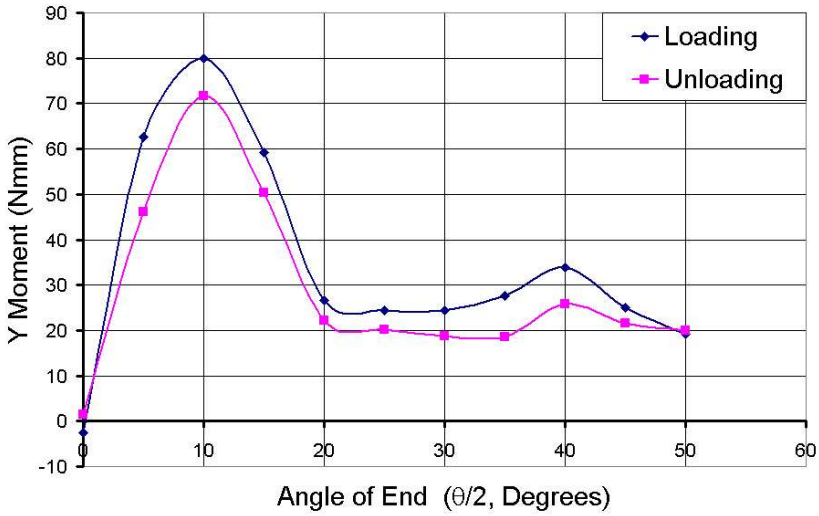

Figure 13. Experimental Moment-Rotation Relationship for an Equal Sense Bend

state moment result of -23.25Nmm. It is known that the basic theory steady state moment of -21.86Nmm is an under approximation, as the theory assumes an infinitely long tape spring (neglecting end effects), so an experimental value of around -23Nmm is a realistic result. It is also shown that the complex shell theory result tends to match M_{-}^{*} closer than M_{-}^{max}. This is an expected result, as the same phenomenon can be found in Seffen et al. (2000). The developed complex theory predicts the steady state moment to be -21.43Nmm which is again an under approximation of the experimental result.

By studying the peak moments predicted from the finite element models it can be seen that model one suggests a peak moment of -67.2Nmm whereas model two suggests -107Nmm. This is because model one is a torsional model, attempting to force a failure in the torsional mode. However, as it begins to reach the peak moment it twists instead of buckling resulting in a low peak moment. Model two is the minimum peak moment for a 'snap through' failure, therefore the finite element data suggests that the equal sense, peak moment lies between -67Nmm and -107Nmm. With a peak moment of -80Nmm the experimental result lies in the centre of this range, suggesting that this is an accurate result.

From the 2D opposite sense bend results in table 2 it can be seen that the experimental result predicting M_{+}^{*} is very close to the theoretical values. Unfortunately, no experimental results were produced for the opposite sense peak moment, however, both finite element models predict a value of just over 340Nmm and the analytical model suggest a value of 248.4Nmm. From previous work on two dimensional bends it has been found that finite element models have tended to predict the opposite sense peak moment with an error of less than 6% from the experimental result, whereas the analytical model is a considerable under-approximation of the true result (Seffen et al., 2000). This suggests that the true opposite sense, peak moment is around 340Nmm.

It can be seen from the previous data that the all the experimental results produced tend to agree with the

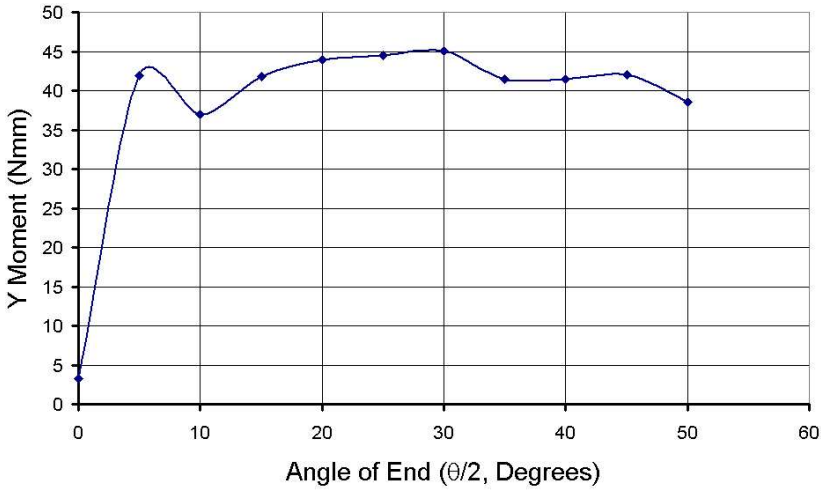

Figure 14. Experimental Moment-Rotation Relationship for an Opposite Sense Bend

Result Method	M_{-}^{max} (Nmm)	M_{-}^{*} (Nmm)
Experimental	-80.0	-23.25
Basic Theory	-	-21.86
Complex Theory	-20.46	-
Developed Complex Theory	-	-21.43
FEA Model 1	-67.2	-
FEA Model 2	-108.0	-22.68

Table 1. 2D Equal Sense Bend Results Summary

Result Method	M_{+}^{max} (Nmm)	M_{+}^{*} (Nmm)
Experimental	-	41.75
Basic Theory	-	40.60
Complex Theory	248.4	35.47
Developed Complex Theory	-	38.11
FEA Model 1	340.0	-
FEA Model 2	343.5	-

Table 2. 2D Opposite Sense Bend Results Summary

theoretical predictions. This implies that the measurement system and the design of the test rig is very capable of producing accurate data, allowing confident experimental analysis of the more complex, three dimensional tape spring bends.

5. THREE DIMENSIONAL RESULTS AND COMPARISONS

For the three dimensional experimental tests one Y SGU (with the same properties as shown in section 4) was used per y axle and one X' SGU was used per x'axle. Each X' SGU incorporated a Nickel Silver metal strip 6mm wide, 0.4mm thick with an SGU arm length of 18mm. Because of the anticipated high twist reaction moments of a three dimensional opposite sense bend the initial tests were limited to equal sense, three dimensional bends. All tests were performed with an ideal bend twist relationship. I.e. the twist angle throughout the tests would remain twice as large as the bend angle. This results in a final longitudinal bend (θ) of 90° and a total twist angle (γ) of 180°.
The experimental results are displayed in figures 15 and 16. Theoretical results derived from shell theory analysis methods have been overlayed on these experimental curves to allow a direct comparison between the two sets of results.
The theoretical model is based on the shell theory analysis approach shown in Mansfield (1973), focusing on post buckling analysis. By making some assumptions about the curvature of the three dimensional fold, the rotation of the lines of principle curvature of the folded surface, as the twist increases, can be modelled accurately. Using this data the reaction moments can be modelled for all post buckling values of θ and γ.
It can be seen from figure 15 that the experimental longitudinal moment rises to a peak moment of -63Nmm,

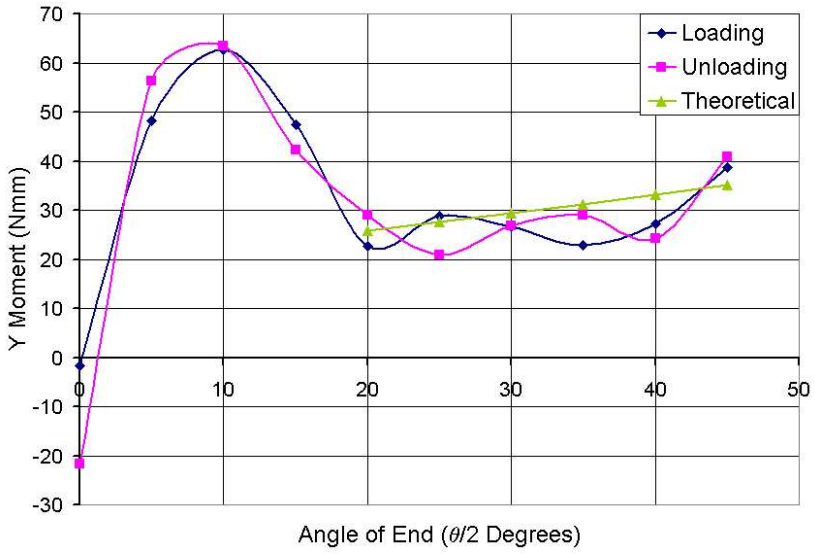

Figure 15. Graph of 3D equal sense longitudinal moment overlayed with theoretical result

which is a lower peak moment than the two dimensional result. This is expected as it is known that as equal sense bends fail in the torsional mode, therefore the presence of twist initiates buckling at a lower moment magnitude. By averaging the steady state moments it is found that the three dimensional steady state moment is predicted to be -28Nmm, which is high than the two dimensional result. This is due to the fact that, as γ increases the steady state moment also increases resulting in a higher average moment magnitude. This can be seen clearly in the experimental curve as compared to the two dimensional equal sense curve. The theoretical rise in the moment closely approximates the experimental result at $\theta = 40°$ and $\theta = 90°$, however tends to over approximate the moment between these values of θ. Although, the experimental results over this range tend to rise and fall suggesting slight experimental inaccuracies over this region.
It is known from finite element models that tape springs subjected to a pure twisting moment has an approximately linear torque-rotation relationship. However from the experimental results shown in figure 16 it can be seen that, for an ideal three dimensional bend, the torque-rotation relationship follows an 's' shape, flattening out when $\gamma = 0°$ and $\gamma = 180°$. It can also be seen from figure 16 that the loading curve rises at both $\gamma = 20°$ and $\gamma = 80°$, whereas the unloading curve is a smooth change in moment back to 0° rotation. This is due to the tape buckling at different twist angles when the rotational displacements were applied. Although it is not obvious from the graph, it is known that the theoretical model does follow the 's' shape trend. However, the experimental results clearly accent this trend to a higher degree. In general, the theoretical model is a good prediction of the experimental results as the theoretical curve remains consistently close to the experimental

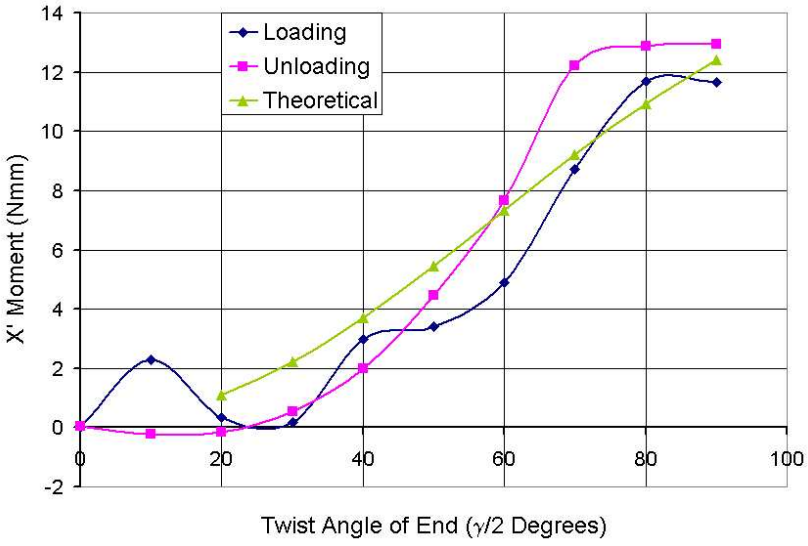

Figure 16. Graph of 3D equal sense twist moment overlayed with theoretical result

torque-rotation relationship.
Some experimental sources of error have been identified are are currently being rectified for all future experimental tests. These errors include optimisation accuracy of the SGU's, unwanted 'spring' moments from the strain gauge wires and circuit failures. However, it can be seen from all the comparative results that the test rig has met its design requirements and has produced accurate experimental data.

6. CONCLUSION

This research study has focused on the design and development of an experimental test rig to statically analyse three dimensional tape spring bends. Such tape spring configurations have a wide variety of future space applications and this work is the first step to model the dynamic nature of such folds. To verify the accuracy of the experimental method, the two dimensional fold results have been compared with established theoretical analysis methods concluding that the test rig is very capable of producing accurate and reliable results. This test rig is then used to analysis three dimensional tape spring folds and directly compared with new theoretical models. These models have been developed from shell theory to simulate both the bending and twisting static reaction moments produced from post buckling tape spring folds. Future work will focus on using such models to independently studying the longitudinal and twisting dynamic systems. Damping can then be used to simulate the presence of a blanket array, modelling the deployment of the array system. However, from this work it was found that there was a very good correlation between the experimental and theoretical three dimensional results, validating the theoretical model and resulting in an excellent foundation for future dynamic analyses of the complete system.

REFERENCES

Liebe C.C., Mobasser S., MEMS based sun sensor, IEEE Aerospace Conference Proceedings, 2001, V3, p31565-31572

Fleeter R., The Logic of Microspace, Microcosm/Kluwer, 2000, ISBN: USA 1-881-883-11-6, UK 0792360281

Paine M.D., Gabriel S.B., A micro-fabricated colloidal thruster array, AIAA paper 2001–3329

Walker S.J.I., Aglietti G.S., An application of Tape Springs in Small Satellite Area Deployment Devices, Proceedings of 5th International Conference on Dynamics and Control of Systems and Structures in Space, 2002

Seffen K.A., You Z., Pellegrino S., Folding and deployment of curved tape springs, International Journal of Mechanical Sciences, 2000, V42, p2055-2073

Seffen K.A., Pellegrino S., Deployment dynamics of tape springs, Proc. Roy. Soc. Lond., 1999, A.455, p1003-1048

Mansfield E.H., Large-deflection torsion and flexure of initially curved strips, Proc. Roy. Soc. Lond., 1973, A.334, p279-298